Adsorption of murexide dye from aqueous solution using a novel Schiff base tin(IV) compound

Seda Karayünlü Bozbaş*, Begüm Canan Yıldız Aras, Muhammed Karabulut, Asgar Kayan

Kocaeli University, Faculty of Art and Science, Department of Chemistry, 41380 Kocaeli, Turkey, Tel. +90 262 3032020; Fax: +90 262 3032003; email: sedak@kocaeli.edu.tr/sedakarayunlu@hotmail.com (S.K. Bozbaş) ORCID ID: https://orcid.org/ 0000-0002-5177-3826; emails: bcanan89@gmail.com (B.C. Yıldız Aras), muhammedd.ahmett@gmail.com (M. Karabulut), akayan@kocaeli.edu.tr (A. Kayan)

ABSTRACT

In this study, the synthesis of an easily synthesized, non-toxic and inexpensive material and its use in dye removal have been demonstrated. The synthesis of novel material, tin(IV) chelate compound, was carried out using simple and inexpensive Schiff base ligands. This novel material was used for the first time as an adsorbent to remove murexide dye from a model aqueous solution. ^{1}H-NMR, ^{13}C-NMR, Fourier-transform infrared spectroscopy, MS, and elemental analysis techniques were performed for the characterization of the new tin-based adsorbent and the open structure of the compound was proposed. Murexide dye removal from a model aqueous solution was performed by examining five important factors of adsorption. Batch adsorption is the easiest way to remove dyes at a low cost. The optimum parameter values to maximize the adsorption efficiency were obtained at pH 3, 100 mg/L dye concentration, 20 min of contact time, 40 mg adsorbent dose, and 25°C. The highest adsorption recovery value and the adsorption capacity found at optimum parameters were 99.00%, and 248.8 mg/g, respectively. Three adsorption isotherms were calculated at 25°C. The highest R^2 value was found at 0.99 for the Langmuir isotherm model, the adsorption kinetic obeyed the pseudo-second-order kinetics, and the thermodynamic data suggested a spontaneous and exothermic process.

Keywords: Murexide removal; Schiff base; Tin; Langmuir; Kinetics

1. Introduction

Water is one of the main crucial components of life and is vital for all living things on earth. It is impossible to think of a life without water. Unfortunately, due to the uncontrolled development of the industry and industrial wastes released to the environment, water resources are being rapidly polluted. Conscious or unconscious discharge of dyes into the aqueous environment causes the aquatic environment to have an undesirable and unnatural color, thus reducing the penetration of sunlight. Also, some dyes are inherently toxic [1–3]. Dye materials with significant coloring capacity are widely used in many industry areas like textile, food, plastic, paper and pulp, etc. [1,2,4]. Most of these dye compounds are toxic to animals, plants, and human beings. To find a solution to this issue, removing dyes from the aqueous solution has been studied and as a result, various techniques such as adsorption, chemical precipitation, ion exchange, membrane systems, and several advanced techniques like electrocoagulation, photocatalysis, and advanced oxidation processes [5,6] have been used to remove dyes from aqueous solutions. Among these methods, adsorption is widely preferred in the purification of water because it is efficient, simple, and fast and its cost is

* Corresponding author.

low as well [7,8]. During the adsorption process, the choice of adsorbent greatly affects the adsorption selectivity and capacity [7–9]. A wide range of compounds was used as an adsorbent to remove dyes from the aqueous solution [10,11]. Some materials like zeolites, activated carbon, ion exchange resins, polymers, and natural wastes [12,13] which were frequently used as adsorbents in previous studies, have limited applications due to their poor selectivity and low adsorption capacity [14]. Unlike these, Schiff base metal compounds have better adsorptive properties for removing dyes from aqueous solutions. Therefore, new Schiff base adsorbents containing oxygen and nitrogen atoms have been investigated for the removal of dyes from aqueous solutions because they can easily form a complex with central metal ions [15]. The new nanohybrid material containing Cd(II) semicarbazone Schiff base complex was synthesized by Farhadi et al. [16]. This nanohybrid was tested as an adsorbent to remove cationic dyes such as Methylene blue (MB) and Rhodamine B (RhB), as well as anionic dye Methyl orange (MO) and it was mentioned that the novel material had an excellent adsorption ability towards these dyes. The removal of MO from aqueous solution performed by nano-composite containing cobalt (Si/Al-PAEA = SA@Co) was proved in the study of Arshadi [17].

Murexide (MX) is a dye used as an indicator in EDTA titrations and dyes wool and many textile products. Murexide is also used as a colorimetric reagent for the measurement of strontium, lead, nickel, copper, zinc, and cadmium [18]. The chemical formula of murexide is $C_8H_8N_6O_6$ and this dye is also known as ammonium purpurate. It is toxic and can be dangerous to the eyes, skin, and respiratory tract on exposure. When murexide dye is used in industry, a significant part of it mixes with wastewater which poses a danger to aquatic organisms as well as for humans and animals [19].

This study aims to understand the murexide dye adsorption from a model aqueous solution by using Schiff base tin adsorbent. In recent years, there has been a considerable amount of increase in the synthesis and use of new materials in the removal of dyes and heavy metals. However, the synthesis methods of these new materials are generally costly, require relatively complex and sophisticated technology, and may include toxic starting materials, which can limit their use. In this work, 2-((E)-(p-tolylimino)methyl)phenol (TIMPH) ligand was reacted with butyltin trichloride to form a Schiff base tin compound. This tin compound was characterized by a combination of spectroscopic techniques such as ¹H-NMR, ¹³C-NMR, Fourier-transform infrared spectroscopy (FTIR), MS, and elemental analysis. A series of batch experiments were conducted to evaluate the effect of murexide dye adsorption onto the Schiff base tin adsorbent from a model aqueous solution under the different experimental parameters. Moreover, the isotherms, kinetics, and thermodynamic results of the adsorption process were determined and evaluated.

2. Experimental

2.1. Materials

Salicylaldehyde (98%, Sigma-Aldrich), p-toluidine (99%, Merck), ethyl alcohol absolute (Merck), butyltin trichloride (95%, Sigma-Aldrich), murexide (ACS reagent, Merck), and *n*-hexane (95%, Merck) were used as received. HCl and NaOH were of analytical grade. All glassware was kept in an acidic washing solution for at least one night before being used and then rinsed with deionized water. The deionized water was supplied from the Elga brand with 18.2 μs of conductivity.

2.2. Instruments

¹H and ¹³C-NMR spectra of TIMPH ligand and tin compound were measured on a Bruker 400 MHz NMR spectrometer (100 MHz for ¹³C and 400 MHz for ¹H). FTIR spectra were recorded from 400–4,000 cm⁻¹ on an Alpha-P Bruker spectrophotometer. LECO CHNS-932 elemental analyzer was employed to determine carbon, hydrogen, and nitrogen amounts in both TIMPH ligand and tin compound. High-resolution mass spectra (HRMS) were recorded on a Waters SYNAPT G1 MS spectrometer using electrospray ionization (ESI±, in the range of 50–1,100 Da). The absorbance of dye after adsorption process was measured using a UV-Vis spectrophotometer (T80 + UV/VIS Spectrometer PG Instruments Ltd). The pH of dye solutions was measured by Hanna Instruments pH 211 Microprocessor. In the method of adsorption, several brands of magnetic stirrers were used.

2.3. Synthesis of 2-((E)-(p-tolylimino)methyl)phenol

Salicylaldehyde (4.00 g, 0.032 mol) was added to the stirring solution of p-toluidine (3.45 g, 0.032 mol) in 25 mL of ethyl alcohol and the reaction was allowed to react at 80°C for 3 h. The resulting mixture was cooled to approximately 20°C and an orange solid precipitate was obtained. Then, the precipitate was filtered, washed two times with 20 mL ethanol and dried under reduced pressure by a vacuum evaporator as in Kayan [20]. Elemental analysis of $C_{14}H_{13}NO$ (211.26 g/mol) Calculated: H 6.20, C 79.59, N 6.63%; Found: H 6.28, C 79.35, N 6.42. HRMS (±ESI) (m/z): [$C_{14}H_{13}NO$] = 212.0 (100%) Da. ¹H NMR (400 MHz, CDCl₃), δ (ppm): 2.42 (s, 3H, CH₃); 6.90–7.45 (m, 8H, Ar); 8.68 (s, 1H, CH); 13.30 (s, 1H, OH) ppm. FTIR (cm⁻¹): 3,050; 3,020; 2,860; 1,618 (C=C, Ar); 1,598 (C=C, Ar); 1,576 (C=N) ; 1,510; 1,496; 1,460; 1,416; 1,368; 1,280 (C–O, phenolic); 1,180; 1,160; 1,120; 1,032; 912; 850; 836; 790; 754; 632.

2.4. Synthesis of [SnBuCl₃(TIMPH)₂] compound

The obtained TIMPH ligand (0.64 g, 3.0 × 10⁻³ mol) was added to the solution of BuSnCl₃ (0.45 g, 1.50 × 10⁻³ mol) compound in 30 mL of ethyl alcohol. This mixture was stirred at ambient temperature for 3 h and it gave yellow product. Then, a vacuum evaporator was used to remove the solvents from mixture at 35°C. The resulting compound was then washed two times with 20 mL n-hexane and dried under vacuum. Elemental analysis, ($C_{32}H_{35}Cl_3N_2O_2Sn$, M_w = 704.70 g/mol) Calculated: H 5.01, C 54.54, N 3.98%. Found: H 4.57, C 54.77, N 4.33%. ¹H-NMR (400 MHz, CDCl₃), δ (ppm): 0.92 (s, 3H, α-CH₃, Bu); 1.27 (m, 2H, γ-CH₂, Bu); 1.44 (m, 2H, β-CH₂, Bu); 1.86 (t, 2H, α-CH₂, Bu); 2.41 (s, 6H, CH₃-Ar); 6.91–7.51 (m, 16H, C₆H₄); 8.52 (s, 2H, CH=N); 9.92

(s, H, OH), 11.0 (s, H, OH). ^{13}C-NMR, (100 MHz, CDCl$_3$), δ (ppm): 13.5 (CH$_3$); 20.9 (γ-CH$_2$); 21.2 (CH$_3$); 25.6 (β-CH$_2$); 27.1 (α-CH$_2$); 117.9, 118.8, 120.5, 130.0, 130.4, 133.9, 136.2, 138.6 (=C, Ar); 160.7 (C–OH, Ar), 165.3 (CH=N). FTIR (cm^{-1}): 3,044 (C–H, Ar, sp^2, *asym*), 2,947 (C–H, sp^3, *asym* str), 2,868 (C–H, sp^3, *sym* str), 1,637 (C=C, Ar), 1,601 (C=C, Ar), 1,543 (CH=N), 1,484 (C–H, sp^3, bending), 1,379; 1,284 (C–O, phenolic), 1,244; 1,188; 1,147; 1,016; 897; 817; 790; 754; 686; 623. MALDI-TOF MS (m/z): [C$_{32}$H$_{35}$Cl$_3$N$_2$O$_2$Sn+Na]$^+$ = 729.01 (100%), 731.02 (90%) and 727.02 (97.8%) Da.

2.5. Adsorption experiments on [SnBuCl$_3$(TIMPH)$_2$] compound

The murexide dye adsorption was investigated on different amounts (10–60 mg) of Schiff base tin compound in batch adsorption mode. The experiments were performed in 250 mL Erlenmeyer flasks containing 100 mL of murexide dye solution with different initial concentrations (100–600 mg/L). These solutions were agitated with the magnetic stirrer at 300 rpm, at a different initial temperature (25°C–65°C), and in contact times (10–80 min.). The solution's pH (2–10) was adjusted by a pH meter with a negligible volume of 0.1 M HCl and NaOH before adsorption. At the end of the equilibrium period, the suspension was centrifuged for 3 min at 4,000 rpm. The concentration of murexide dye in the filtrate taken by decantation was measured by a T80 + UV/VIS spectrophotometer at the maximum wavelength of 525 nm. In Eqs. (1) and (2), the percentage of removal and the amount of equilibrium adsorption capacity were given.

$$ \%R = \left(\frac{C_0 - C_e}{C_0} \right) \times 100 \tag{1} $$

$$ q_e = \frac{(C_0 - C_e)V}{w} \tag{2} $$

where C_0 and C_e are the initial dye concentration (mg/L) and the equilibrium dye concentration (mg/L), respectively.

2.6. Adsorption isotherms, kinetics, and thermodynamics

2.6.1. Isotherms

The parameters obtained from various isotherm models provide valuable details on the essence of the adsorption process interaction, the surface properties of the adsorbent, and their adsorbent affinity [21]. The isotherms that depend on equilibrium conditions at a constant temperature were plotted on graphs. For the newly synthesized adsorbent, the most popular adsorption isotherms (Langmuir, Freundlich, and Temkin isotherms) were investigated for murexide dye. The three-isotherm equations are shown in Table 1.

By linear form, the Langmuir isotherm model was determined. In Table 1, the maximum monolayer adsorption capacity of the adsorbent is Q_{max} (mg/g), and K_L is the Langmuir adsorption constant (L/mg). The Q_{max} and K_L were calculated from the intercept and slope of the linear plot [19–22]. The adsorption properties of heterogeneous surfaces were also represented using the Freundlich isotherm.

The Freundlich isothermal constants of adsorption capability and adsorption strengths are K_F (L/mg) and n_f, respectively. From the linear plot equation, these values were determined. Due to the adsorbent/adsorbate interactions, the Temkin isotherm accepts a linear decrease in the adsorption temperature of all molecules in the layer. In the Temkin isotherm model, the Temkin isotherm equilibrium binding constant (L/g) is K_T and the heat-related constant (J/mol) is B. The values of K_T and B are computed from the plot of q_e against $\ln C_e$ [23,24].

2.6.2. Adsorption kinetics

This study used the pseudo-first-order kinetic model and the pseudo-second-order kinetic model among the several kinetic models to describe the adsorption rate and the adsorption mechanism of murexide dye on the Schiff base tin compound. These kinetic equations and coefficients used are demonstrated in Table 2.

where q_e (mg/g) is the equilibrium adsorption capacity, q_t is the adsorption capacity at time t (mg/g), t is time (min), k_1 (min^{-1}) and k_2 (g/mg min) are the pseudo-first-order rate and pseudo-second-order rate constants, respectively. From the slope and intercept of the log graph ($q_e - q_t$) against time t, the pseudo-first-order rate constant (k_1) and equilibrium adsorption power (q_e) were determined. The pseudo-second-order rate constant k_2 and the equilibrium adsorption capability (q_e) values were determined from the intercept and the graph slope of t/q_t against time t [25].

2.6.3. Adsorption thermodynamics

One of the other essential considerations for identifying and recognizing the meaning of adsorption is thermodynamic analysis. Van't Hoff equation describes the change in the equilibrium constant with the effect of temperature. The thermodynamic parameters of the equations including the change in Gibbs free energy (ΔG°), the change in enthalpy (ΔH°), and the change in entropy (ΔS°) values were

Table 1
Isotherm equations

Isotherms	Equations	Plot
Langmuir	$\dfrac{C_e}{q_e} = \left(\dfrac{1}{K_L Q_{max}} \right) + \left(\dfrac{C_e}{Q_{max}} \right)$	C_e/q_e against C_e
Freundlich	$\ln q_e = \ln K_f + \dfrac{1}{n_f}(\ln C_e)$	$\ln q_e$ against $\ln C_e$
Temkin	$q_e = B \ln K_T + B \ln C_e$	q_e against $\ln C_e$

Table 2
Kinetic equations

Pseudo-first-order equation	Pseudo-second-order equation
$\log(q_e - q_t) = \log q_e - \left(\dfrac{k_1}{2.303} \right) \times t$	$\dfrac{t}{q_t} = \dfrac{1}{k_2 (q_e)^2} + \left(\dfrac{1}{q_e} \right) \times t$

calculated from the equations of 3–4 [26]. These values were used to assess the thermodynamic feasibility of the effect of temperature on the process of adsorption.

$$\ln K_c \left(\frac{\Delta S^\circ}{R} \right) - \left(\frac{\Delta H^\circ}{RT} \right) \tag{3}$$

$$\Delta G^\circ = -RT \ln K_c \tag{4}$$

where K_c (q_e/C_e) is the thermodynamic equilibrium constant, R is the universal gas constant (8.314 J/mol K), and T is the absolute temperature of the solution.

3. Results and discussion

3.1. Schiff base tin adsorbent

The stoichiometric reaction between p-toluidine and salicylaldehyde in a 1:1 mole ratio in ethanol at 80°C produced a TIMPH ligand as in the literature [20]. The reaction of BuSnCl$_3$ with TIMPH in the 1:2 mol ratio in ethanol gave the tin compound at room temperature. The formulation of tin compound was based on mass measurements, elemental analysis, the interpretation of ^{1}H, ^{13}C-NMR, and FTIR spectra. TIMPH ligands were coordinated to the tin atom at two sites via both O and N atoms. In the ^{1}H-NMR spectrum of tin compound, two OH protons were shifted from 13.0 ppm for free ligands to 9.92 (s, H, OH), and 11.0 (s, H, OH) ppm. This shift showed that OH protons were protected in the tin compound and OH groups were interacted with the tin atom to a different degree. FTIR measurement showed that a strong peak was observed at 1,576 cm^{-1} in the spectrum of TIMPH ligand for the C=N group. After the coordination of TIMPH to tin atom, the C=N peak was shifted to the lower value (1,543 cm^{-1}) in the spectrum. It is an expected phenomenon that the bonding of the CH=N group to the metal atom lowers the double bond character of the CH=N group [27]. In the ^{13}C-NMR spectrum of tin compound, the C–OH (160.7 ppm) and CH=N (165.3 ppm) carbons having different values than the peaks of the TIMPH ligand indicated that there was a binding as shown in Fig. 1.

The spectroscopically proposed structure was also confirmed by mass measurement. The peak at 729.01 (100%), 731.02 (90%), and 727.02 (97.8%) Da on mass spectrum confirmed the proposed structure ([C$_{32}$H$_{35}$Cl$_3$N$_2$O$_2$Sn+Na]$^+$).

3.2. Effect of pH in the removal of murexide dye

The pH of aqueous solutions is an important parameter that controls the adsorption process. The surface charges of the adsorbent are controlled by the initial pH [19,28,29]. The effect of the initial pH on the percentage removal of murexide in the pH range from 2 to 8 at room temperature (100 mg/L murexide) by using 40 mg of the adsorbent at a contact time of 20 min was shown in Fig. 2. It was observed that the maximum percentage removal of murexide on Schiff base tin adsorbent was obtained at pH 3.0 and its value was determined to be 99.82%. Maximum adsorption occurred in an acidic environment. In the literature research, it has been observed that activated carbon adsorbs high amounts of murexide at low (acidic) pH 2 [30]. Therefore, all subsequent studies were performed at low pH 3. In an acidic environment, adsorbents are protonated and have a positive charge to attract anionic dye ions to their surface, which increases dye removal. However, in the case of neutral pH, the percentage of dye removal is reduced. This is because at high pH, the adsorbent is covered with negative charges on the surface causing a repulsive force on the dye. The reason for the maximum removal of murexide dye used in this study at acidic pH was due to the presence of polar covalent, coordinated covalent bonds between the tin atom of Schiff base compound and the dye ions in addition to attractive forces [31,32].

3.3. Effect of initial dye concentration on adsorption

The initial dye concentration may have different effects on adsorption. Therefore, in this study, the effect of initial dye concentration on adsorption was investigated. Adsorption of murexide onto [SnBuCl$_3$(TIMPH)$_2$] was
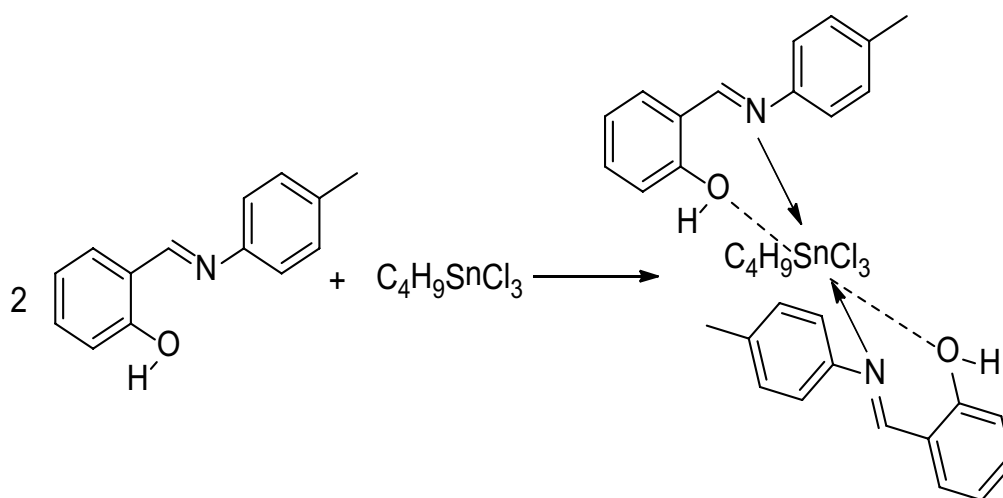

Fig. 1. Structure of [SnBuCl$_3$(TIMPH)$_2$] compound.

carried out at different initial dye concentrations ranging from 100 to 600 mg/L, and other conditions such as time (20 min), pH (3), temperature (25°C), and amount of adsorbent (40 mg) were kept constant. Fig. 3 shows the effect of initial murexide dye concentration on dye removal percentage. The maximum adsorption removal percentage was 98.52% for a 100 mg/L concentration of dye solution. The high percentage of dye removal at a low concentration of dye could be attributed to the presence of active sites in the adsorbent. And the rise in the initial concentration of dye could be caused by a reduction in the driving force of the concentration gradient [33–35].

3.4. Effect of adsorbent amount

By preparing an adsorbent–adsorbate solution, the effect of the amount of adsorbent on the adsorption process can be achieved by applying a different amount of adsorbent to the solution at a constant initial dye concentration and shaking it until equilibrium time [36,37]. The effect of different adsorbent amounts on murexide adsorption was investigated. Fig. 4 represents the results. It was found that as the adsorbent dose increased, the adsorption value increased. The maximum adsorption value for the 60 mg dose was 99.5%. This is because as the amount of adsorbent increases, the active surface areas of the adsorbent and adsorption areas increase [38,39]. 40 mg of

$[SnBuCl_3(TIMPH)_2]$ was selected as the optimum amount of adsorbent.

3.5. Effect of temperature

The experimental findings indicate that the temperature is a critical factor that greatly affects the adsorption process. To establish whether the continuous adsorption process was endothermic or exothermic in the dye adsorption process, dye adsorption experiments were performed at temperatures of 25°C–65°C for 100 mL of 100 mg/L murexide, pH 3, 40 mg adsorbent dosage, and 20 min contact time. Fig. 5 indicates that the maximum percentage removal of murexide at 35°C was 99.5%. At higher temperatures, the adsorption capacity can increase or decrease depending on the nature of the reaction and other controlling variables. Adsorption can increase at higher temperatures if the reaction process is endothermic. The increased surface coverage at higher temperatures, as well as the expansion and formation of reactive and active sites, may explain this. When a reaction is exothermic, the amount of adsorption decreases as the temperature rises [40,41].

3.6. Effect of time

The effect of contact time on the percentage removal of murexide dye with an initial concentration of 100 mg/L
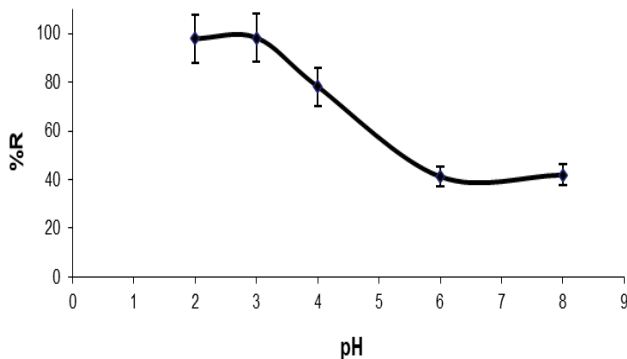

Fig. 2. Effect of pH on the adsorption of murexide onto [SnBu-Cl₃(TIMPH)₂] (Temperature: 25°C; initial dye concentration: 100 mg/L; adsorbent dose: 40 mg; time: 20 min).
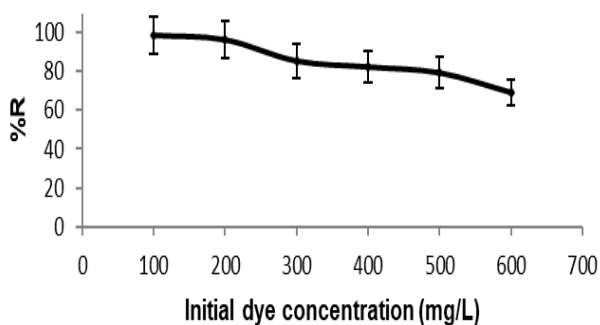

Fig. 3. Effect of initial dye concentration on adsorption (Adsorbent dose: 40 mg; temperature: 25°C; pH: 3; time: 20 min).
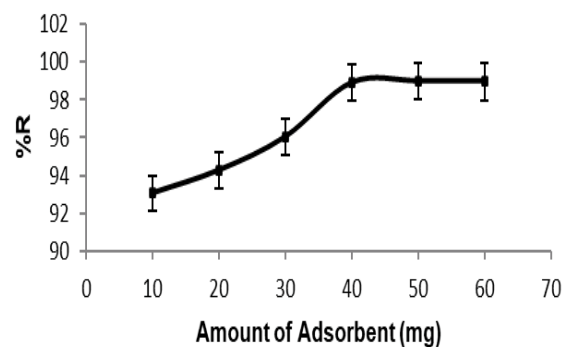

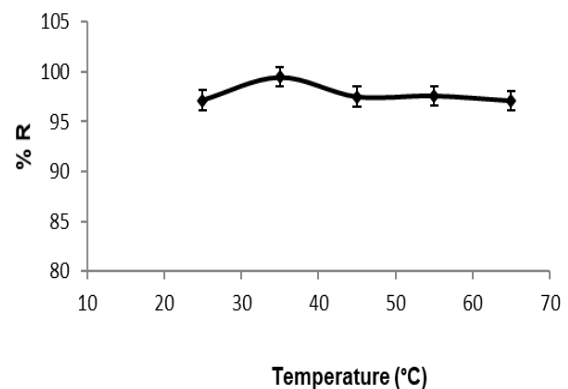Fig. 4. Effect of adsorbent amount (Dye concentration: 100 mg/L; temperature: 25°C; pH: 3; time: 20 min).

Fig. 5. Effect of temperature (Dye concentration: 100 mg/L; pH: 3; time: 20 min).
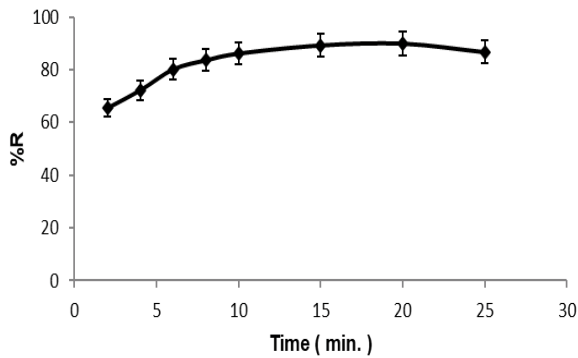
Fig. 6. Effect of time (Dye concentration: 100 mg/L; temperature: 25°C; pH: 3; adsorbent dose: 40 mg).

was tested at pH 3 at 25°C. It has been observed that the removal of dye increased on $[SnBuCl_3(TIMPH)_2]$ adsorbent with increasing contact time and achieved the highest value (Fig. 6). It is almost constant with an increase in contact time after 20 min depending on the findings [42].

3.7. Adsorption isotherms

Adsorption isotherms are very important because they can explain the interactions between the dye molecules and adsorbent. In this study, the suitability of experimental data to Langmuir, Freundlich and Temkin isotherm models was investigated to determine the adsorption mechanism between dye molecules and adsorbent. Three isotherms are plotted in Fig. 7 and the values calculated from the isotherm equations are presented in Table 3.

The equilibrium data better matched the isotherms of Langmuir adsorption than the isotherms of Temkin. R^2 (correlation coefficient) value of linear equation was 0.99, which clearly suggested that Langmuir isotherm was good to explain adsorption of murexide on $[SnBuCl_3(TIMPH)_2]$. In a monolayer and by chemisorption, there has been an adsorption of murexide dye on $[SnBuCl_3(TIMPH)_2]$ adsorbent [43]. The calculated maximum adsorption capacity of murexide dye on $[SnBuCl_3(TIMPH)_2]$ adsorbent was about 200 mg/g and this value was not far from our experimental maximum adsorption capacity value which was 248.8 mg/g.

The Freundlich adsorption isotherms R^2 value was 0.97, and the adsorption favorability and high adsorption preference of murexide dye onto $[SnBuCl_3(TIMPH)_2]$ adsorbent was shown to be $1/n$ (0.29) [23,28].

3.8. Adsorption kinetics

The murexide dye adsorption control rate mechanism on $[SnBuCl_3(TIMPH)_2]$ compound was investigated by fitting pseudo-first-order and pseudo-second-order models. To gain knowledge about the character of adsorption, kinetic studies were carried out. The linear plots of the pseudo-first-order and pseudo-second-order models are shown in Fig. 8, and the results of the kinetic parameters are shown in Table 4, according to the results of experiments performed at 100 mg/L murexide dye concentrations. From
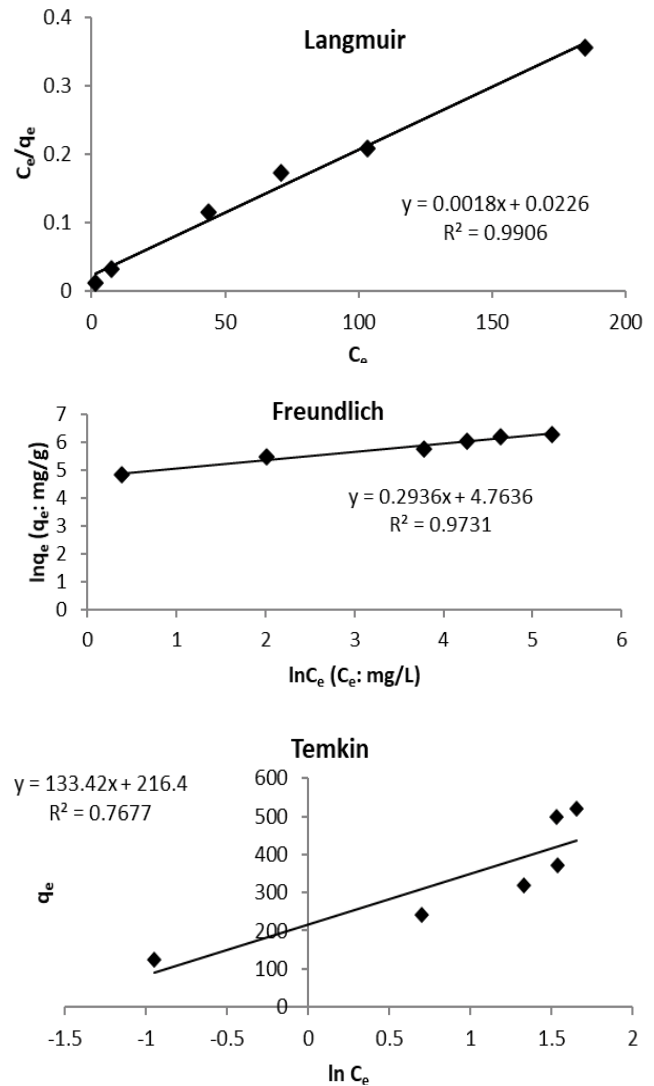

Fig. 7. Langmuir, Freundlich, and Temkin isotherms on $[SnBuCl_3(TIMPH)_2]$ for murexide dye (Temperature: 25°C; pH: 3; adsorbent dose: 40 mg).

Table 4 it can be seen that the $k_2 > k_1$, hence, the pseudo-second-order better represents the adsorption kinetics [44].

The correlation coefficient value R^2 of the pseudo-second-order kinetic equation was 0.99, suggesting that the adsorption reaction may be chemisorption supported by an interaction between the dye and the adsorbent surface [45,46]. The anionic murexide dye can be substituted by chloride ligand in adsorbents. In other words, the ammonium ion (NH_4^+) in murexide dye is replaced with the butyldichlorotin(IV) ion ($C_4H_9SnCl_2^+$) in adsorbent as seen in Fig. 9. Murexide dye also contains nitrogen and oxygen atoms, each of which has lone pair electrons and can serve as a Lewis base against to acidic center. Therefore, both atoms can coordinate to tin atom. In addition to these, it is possible that there are H-bonds, $n-\pi^*$ and electrostatic interactions between murexide dye and adsorbent, as seen in Fig. 9 [47].

Table 3
Adsorption isotherm results for murexide onto [SnBuCl$_3$(TIMPH)$_2$]

	Langmuir constant			Freundlich constant			Temkin constant		
	R^2	Q_{max} (mg/g)	K_L (L/mg)	R^2	K_F (mg/g)	$1/n$	R^2	K_T (L/g)	B
Murexide	0.99	200	37.04	0.95	4.76	0.29	0.77	216.4	133.4
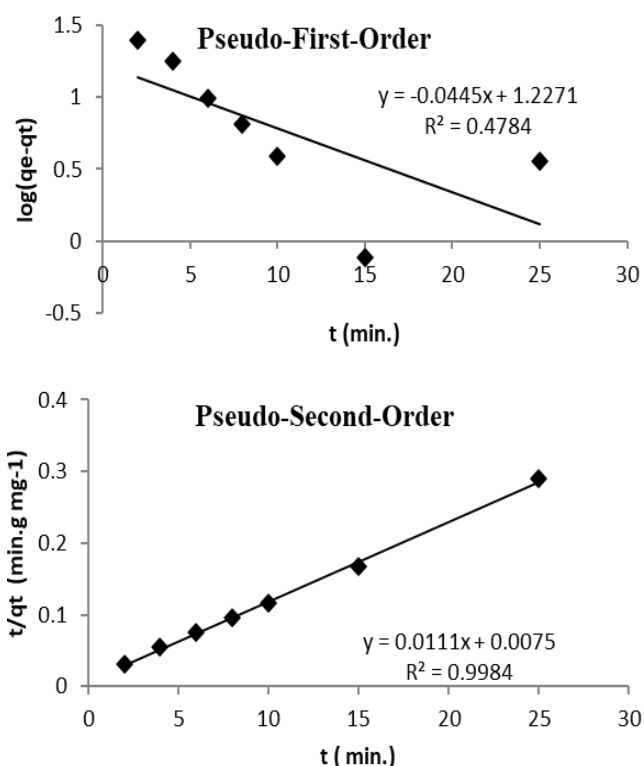
Fig. 8. Pseudo-first-order and pseudo-second-order models kinetic equation for adsorption of metal ions.

The overall work can be summarized as shown in Fig. 10 to make it simple/attractive and easier to understand.

3.9. Thermodynamic parameters of adsorption

To determine the thermodynamic feasibility and spontaneous existence of the process, the thermodynamic constants of the adsorption systems such as change in Gibb's free energy ($\Delta G°$), the change in entropy ($\Delta S°$), and the change in enthalpy ($\Delta H°$), were measured.

Table 5 gives the results of the thermodynamic parameters. In addition, negative values of $\Delta H°$ indicated the exothermic presence of the adsorption process and positive $\Delta S°$ values indicated an increase in the concentration of the adsorbate in the solid phase and an increase in randomness [48,49]. Negative free energy values $\Delta G°$ confirmed the spontaneous existence and feasibility of the adsorption process [50,51].

As a result of this study, it was observed that the newly synthesized Schiff base compound has a high adsorption capacity for murexide dye in a very short time at room temperature. Table 6 shows the comparison of adsorption capacities of several adsorbents including Schiff base tin adsorbent.

As can be seen from Table 6, the [SnBuCl$_3$(TIMPH)$_2$] compound appears to be a more effective adsorbent for murexide dye.

Table 4
Kinetic parameters for murexide adsorption on [SnBuCl$_3$(TIMPH)$_2$]

Dye concentration (mg/L)	Pseudo-first-order kinetic			Pseudo-second-order kinetic		
	R^2	k_1 (1/min)	q_e (mg/g)	R^2	k_2 (g/mg min)	q_e (mg/g)
Murexide (100)	0.478	0.0041	16.87	0.998	0.0164	90.09
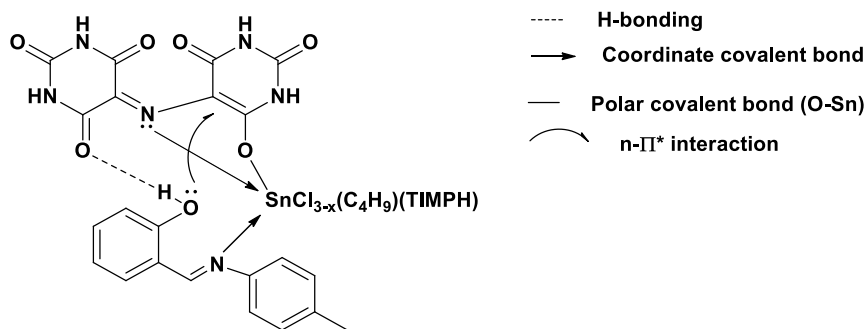
Fig. 9. Bonding between murexide dye and adsorbent.

Table 5
Thermodynamic parameters at different temperatures

T (°C)	$\Delta G°$ (J/mol)	$\Delta H°$ (kJ/mol)	$\Delta S°$ (kJ/mol K)	R^2
25	−56.48			
35	−58.37			
45	−60.27	−0.045	0.189	0.980
55	−62.16			
65	−64.06			

Table 6
Comparison of adsorption capacities of various adsorbents for murexide dye

Adsorbent	Murexide (mg/g)	Reference
Tin oxide nanoparticles loaded on activated carbon (SnO$_2$-NP-AC)	67.00	[13]
Formalin treated *Pisum sativum* peels	11.04	[23]
Rice husk	15.06	[25]
Activated carbon	12.88	[36]
Calcined egg-shell powder	12.64	[37]
HNO$_3$ treated pomegranate bark	1.700	[38]
Lignocellulosic sorbent	15.60	[39]
Cellulosic sorbent	11.80	
(TIMPH)$_2$SnCl$_3$Bu	248.8	This study

3.10. Desorption studies

The dye removal was carried out by using the optimum values at which the maximum adsorption capacity was obtained. The dye-loaded adsorbent obtained after adsorption was investigated for desorption and reuse. For the desorption process, the murexide-loaded adsorbent was mixed in 50 mL of 0.1 M NaOH and HCl solutions for 10 min [47]. The mixtures were then filtered, and then the filtrate was read in a UV-Vis spectrophotometer. The obtained results showed that there was no sufficient desorption because of the strong interaction between the adsorbent and the murexide dye as seen in Fig. 9.

4. Conclusion

In this study, a novel Schiff base tin(IV) compound [SnBuCl$_3$(TIMPH)$_2$] was synthesized, characterized, and used as an effective adsorbent for the removal of murexide dye from aqueous solutions for the first time. Optimization was performed by studying the effects of contact time, initial pH, amount of adsorbent, initial dye concentration, and temperature on [SnBuCl$_3$(TIMPH)$_2$]. The maximum removal percentage (99.00%) and adsorption capacity (248.8 mg/g) were obtained from the results of optimization at pH 3, 100 mg/L murexide dye concentration, 20 min of contact time, 40 mg adsorbent dose, and 25°C. Adsorption equilibrium isotherms were determined and the equilibrium data fitted very well with Langmuir isotherms. The kinetic study of murexide onto [SnBuCl$_3$(TIMPH)$_2$] compound was performed based on pseudo-first-order and pseudo-second-order. The data indicated that the adsorption kinetics follows the pseudo-second-order rate. The determination of the thermodynamic parameters ($\Delta G°$, $\Delta H°$, $\Delta S°$) indicated the spontaneous and exothermic nature of the adsorption process. Studies on dye removal processes are increasing day by day. However, most of these studies are time consuming and costly. This study shows that [SnBuCl$_3$(TIMPH)$_2$] can be used as a low-cost and simply synthesized adsorbent for dye removal. It also showed that [SnBuCl$_3$(TIMPH)$_2$] compound, which has high adsorption capacity and has a high removal rate with fast and easy adsorption process, can be an alternative industrial compound to be applied for the removal of dyes.
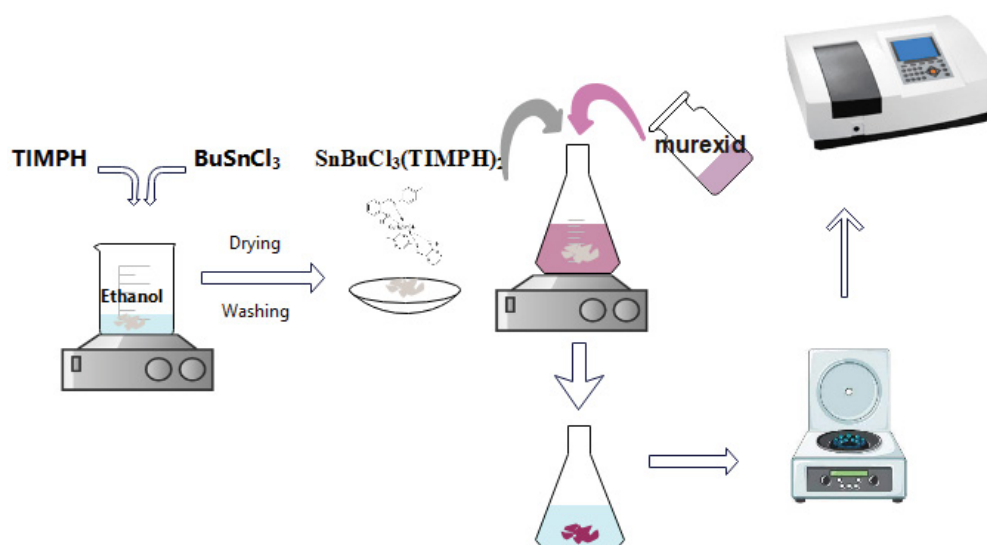

Fig. 10. Summary of overall study.

Availability of data and materials

The datasets generated during and/or analysed during the current study are available from the corresponding author on reasonable request.

References

[1] S. Karayünlü Bozbaş, Y. Boz, Evaluating the optimum working parameters for the removal of Methyl orange from aqueous solution based on a statistical design, Desal. Water Treat., 57 (2016) 7040–7046.

[2] P.A. Carneiro, R.F.P. Nogueira, M.V.B. Zanoni, Homogeneous photodegradation of C.I. Reactive Blue 4 using a photo-Fenton process under artificial and solar irradiation, Dyes Pigm., 74 (2007) 127–132.

[3] L. Huang, M. He, B. Chen, B. Hu, Magnetic Zr-MOFs nanocomposites for rapid removal of heavy metal ions and dyes from water, Chemosphere, 199 (2018) 435–444.

[4] J.E. Hallsworth, Water is a preservative of microbes, Microb. Biotechnol., 15 (2022) 191–214.

[5] A. Ikhlaq, F. Javed, A. Niaz, H.M.S. Munir, F. Qi, Combined UV catalytic ozonation process on iron loaded peanut shell ash for the removal of Methylene blue from aqueous solution, Desal. Water Treat., 200 (2020) 231–240.

[6] N. Noreen, M. Kazmi, N. Feroze, F. Javed, H.G. Qutab, H.M.S. Munir, Treatment of Methylene blue in aqueous solution by electrocoagulation/micro-crystalline cellulosic adsorption combined process, Desal. Water Treat., 203 (2020) 379–387.

[7] D. Bingöl, S. Karayünlü Bozbaş, Removal of lead(II) from aqueous solution on multiwalled carbon nanotube by using response surface methodology, Spectrosc. Lett., An Int. J. Rapid Commun., 45 (2012) 324–329.

[8] S. Karayunlu Bozbas, M. Karabulut, Reusing menengic (*Pistacia terebinthus*) coffee waste as an adsorbent for dye removal from aqueous solution, Int. J. Environ. Anal. Chem., (2021), doi: 10.1080/03067319.2021.1873312 (in Press).

[9] S. Karayunlu Bozbas, U. Ay, A. Kayan, Novel inorganic–organic hybrid polymers to remove heavy metals from aqueous solution, Desal. Water Treat., 51 (2013) 7208–7015.

[10] M. Rafatullah, O. Sulaiman, R. Hashim, A. Ahmad, Adsorption of Methylene blue on low-cost adsorbents: a review, J. Hazard. Mater., 177 (2010) 70–80.

[11] V. Meshko, L. Markovska, M. Mincheva, A.E. Rodrigues, Adsorption of basic dyes on granular acivated carbon and natural zeolite, Water Res., 35 (2001) 3357–3366.

[12] H.M.S. Munir, N. Feroze, N. Ramzan, M. Sagir, M. Babar, M.S. Tahir, J. Shamshad, M. Mubashir, K.S. Khoo, Fe-zeolite catalyst for ozonation of pulp and paper wastewater for sustainable water resources, Chemosphere, 297 (2022) 134031, doi: 10.1016/j.chemosphere.2022.134031.

[13] A. Ikhlaq, H.M.S. Munir, A. Khan, F. Javed, K.S. Joya, Comparative study of catalytic ozonation and Fenton-like processes using iron-loaded rice husk ash as catalyst for the removal of Methylene blue in wastewater, Ozone: Sci. Eng., The J. Int. Ozone Assoc., 41 (2019) 250–260.

[14] R. Zein, R. Suhaili, F. Earnestly, E. Munaf, Removal of Pb(II), Cd(II) and Co(II) from aqueous solution using *Garcinia mangostana* L. fruit shell, J. Hazard. Mater., 181 (2010) 52–56.

[15] A. Naz, S. Arun, S.S. Narvi, M.S. Alam, A. Singh, P. Bhartiya, P.K. Dutta, Cu(II)-carboxymethyl chitosan-silane Schiff base complex grafted on nano silica: structural evolution, antibacterial performance and dye degradation ability, Int. J. Biol. Macromol., 110 (2018) 215–226.

[16] S. Farhadi, M.M. Amini, M. Dusek, M. Kucerakova, F. Mahmoudi, A new nanohybrid material constructed from Keggin-type polyoxometalate and Cd(II) semicarbazone Schiff base complex with excellent adsorption properties for the removal of cationic dye pollutants, J. Mol. Struct., 1130 (2017) 592–602.

[17] M. Arshadi, Adsorptive removal of an organic dye from aqueous solution with a nano-organometallic: kinetic, thermodynamic and mechanism, J. Mol. Liq., 211 (2015) 899–908.

[18] M. Shamsipur, N. Alizadeh, Spectrophotometric study of cobalt, nickel, copper, zinc, cadmium and lead complexes with murexide in dimethylsulphoxide solution, Talanta, 39 (1992) 1209–1212.

[19] S. Davoodi, F. Marahel, M. Ghaedi, M. Roosta, A. Hekmati, A. Jah, Tin oxide nanoparticles loaded on activated carbon as adsorbent for removal of murexide, Desal. Water Treat., 52 (2014) 7282–7292.

[20] A. Kayan, Preparation and characterization of TAMP/TIMP-Ti and Zr compounds and their catalytic activity over propylene oxide and ɛ-caprolactone, J. Turk. Chem. Soc. Sec. A: Chem., 4 (2017) 59–80.

[21] C.S. Araújo, I.L. Almeida, H.C. Rezende, S.M. Marcionilio, J.J. Léon, T.N. de Matos, Elucidation of mechanism involved in adsorption of Pb(II) onto lobeira fruit (*Solanum lycocarpum*) using Langmuir, Freundlich and Temkin isotherms, Microchem. J., 137 (2018) 348–354.

[22] M.R. Awual, M.M. Hasan, M.M. Rahman, A.M. Asiri, Novel composite material for selective copper(II) detection and removal from aqueous media, J. Mol. Liq., 283 (2019) 772–780.

[23] A.A. Edathil, I. Shittu, J.H. Zain, F. Banat, M.A. Haija, Novel magnetic coffee waste nanocomposite as effective bioadsorbent for Pb(II) removal from aqueous solutions, J. Environ. Chem. Eng., 6 (2018) 2390–2400.

[24] R. Lafi, A.B. Fradj, A. Hafiane, B. Hameed, Coffee waste as potential adsorbent for the removal of basic dyes from aqueous solution, Korean J. Chem. Eng., 31 (2014) 2198–2206.

[25] B. Adane, K. Siraj, N. Meka, Kinetic, equilibrium and thermodynamic study of 2-chlorophenol adsorption onto *Ricinus communis* pericarp activated carbon from aqueous solutions, Green Chem. Lett. Rev., 8 (2015) 1–12.

[26] A. Kayan, M.O. Arican, Y. Boz, Ü. Ay, S. Karayunlu Bozbas, Novel tyrosine-containing inorganic–organic hybrid adsorbent in removal of heavy metal ions, J. Environ. Chem. Eng., 2 (2014) 935–942.

[27] B.C. Yildiz, A. Kayan, Ti(IV)-silyliminophenolate catalysts for ɛ-caprolactone and L-Lactide polymerization, Sustainable Chem. Pharm., 21 (2021) 100416, doi: 10.1016/j.scp.2021.100416.

[28] N.Dharmaraj, P. Viswanathamurthi, K. Natarajan, Ruthenium(II) complexes containing bidentate Schiff bases and their anti-fungal activity, Transition Met. Chem., 26 (2001) 105–109.

[29] A. Ikhlaq, T. Aslam, A.M. Zafar, F. Javed, H.M.S. Munir, Combined ozonation and adsorption system for the removal of heavy metals from municipal wastewater: effect of COD removal, Desal. Water Treat., 159 (2019) 304–309.

[30] R. Dhahri, M. Guizani, M. Yılmaz, L. Mechi, A.K. Dhahi Alsukaibi, F. Alimi, Y. Moussaoui, Experimental design analysis of murexide dye removal by carbon produced from waste biomass material, J. Chem., 2022 (2022) 14, doi: 10.1155/2022/9735071.

[31] R. Rehman, T. Mahmud, A. Arshad, Removal of alizarin yellow and murexide dyes from water using formalin treated *Pisum sativum* peels, Asian J. Chem., 27 (2015) 1593–1598.

[32] S.S. Nawar, H.S. Doma, Removal of dyes from effluents using low-cost agricultural by-products, Sci. Total Environ., 79 (1989) 271–279.

[33] R. Rehman, J. Anwar, T. Mahmud, M. Salman, U. Shafıque, W. Zaman, Removal of murexide (dye) from aqueous media using rice husk as an adsorbent, J. Chem. Soc. Pak., 33 (2011) 598–603.

[34] C. Demirbilek, C. Özdemir Dinç, Diethylaminoethyl dextran/epichlorohydrin (DEAE-D/ECH) hydrogel as adsorbent for murexide, Desal. Water Treat., 57 (2016) 6884–6893.

[35] S. Nazir, A. Ikhlaq, F. Javed, Z. Asif, H.M.S. Munir, S. Sajjad, Catalytic ozonation on iron-loaded rice husk ash/peanut shell ash for the removal of erythromycin in water, Environ. Eng. Manage. J., 19 (2020) 829–837.

[36] S. Mam, D.K. Mahmoud, W.A. Karim, A. Irdis, Cationic and anionic dye adsorption by agricultural solid wastes: a comprehensive review, Desal. Water Treat., 280 (2011) 1–13.

[37] K. Bharathi, S. Ramesh, Removal of dyes using agricultural waste as low-cost adsorbents: a review, Appl. Water Sci., 3 (2013) 773–790.

[38] V.K. Garg, R. Gupta, A.B. Yadav, R. Kumar, Dye removal from aqueous solution by adsorption on treated sawdust, Bioresour. Technol., 8 (2003) 121–124.

[39] F. Javed, N. Feroze, A. Ikhlaq, M. Kazmi, S.W. Ahmad, H.M.S. Munir, Biosorption potential of *Sapindus mukorossi* dead leaves as a novel biosorbent for the treatment of Reactive Red 241 in aqueous solution, Desal. Water Treat., 137 (2019) 345–357.

[40] G. Crini, H.N. Peindy, F. Gimbert, C. Robert, Removal of C.I. Basic Green 4 (Malachite Green) from aqueous solutions by adsorption using cyclodextrin-based adsorbent: kinetic and equilibrium studies, Sep. Purif. Technol., 53 (2007) 97–110.

[41] C.S. Lu, Y.L. Chung, K.F. Chang, Adsorption thermodynamic and kinetic studies of trihalomethanes on multi-walled carbon nanotubes, J. Hazard. Mater., 138 (2006) 304–310.

[42] M. Özdemir, Ö. Durmuş, Ö. Şahin, C. Saka, Removal of Methylene blue, Methyl violet, Rhodamine B, Alizarin red, and Bromocresol green dyes from aqueous solutions on activated cotton stalks, Desal. Water Treat., 57 (2015) 18038–18048.

[43] M.W. Ashraf, N. Abulibdeh, A. Salam, Adsorption studies of textile dye (Chrysoidine) from aqueous solutions using activated sawdust, Int. J. Chem. Eng., 1 (2019) 1–8.

[44] A. Birkic, D. Valinger, A. Jurinjak Tušek, T. Jurina, J.G. Kljusuric, M. Benkovic, Evaluation of the adsorption and desorption dynamics of beet juice red dye on alginate microbeads, Gels, 8 (2022) 13, doi: 10.3390/gels8010013.

[45] A. Salama, New sustainable hybrid material as adsorbent for dye removal from aqueous solutions, J. Colloid Interface Sci., 487 (2017) 348–353.

[46] A. Kayan, Inorganic-organic hybrid materials and their adsorbent properties, Adv. Compos. Hybrid Mater., 1 (2019) 34–45.

[47] G.Ö. Kayan, A. Kayan, Polyhedral oligomeric silsesquioxane and polyorganosilicon hybrid materials and their usage in the removal of Methylene blue dye, J. Inorg. Organomet. Polym. Mater., (2022), doi: 10.1007/s10904-022-02288-y (in Press).

[48] A. Shokrollahi, M. Ghaedi, M. Ranjbar, A. Alizadeh, Kinetic and thermodynamic studies of the removal of murexide from aqueous solutions on to activated carbon, J. Iran. Chem. Soc., 3 (2010) 219–235.

[49] A.V. Borhade, A.S. Kale, Calcined eggshell as a cost-effective material for removal of dyes from aqueous solution, Appl. Water Sci., 7 (2017) 4255–4268.

[50] M. Ishaq, K. Saeed, M. Shakirullah, I. Ahmad, S. Sultan, Removal of murexide from aqueous solution using pomegranate bark as adsorbent, J. Chem. Soc. Pak., 34 (2012) 1498–1501.

[51] V. Halysh, O. Sevastyanova, A.V. Riazanova, Walnut shells as a potential low-cost lignocellulosic sorbent for dyes and metal ions, Cellulose, 25 (2018) 4729–4742.